Journal of Applied Polymer Science

An *m*-phenylenediamine-based benzoxazine with favorable processability and its high-performance thermoset

Shitong Ren,[1,2] Xin Yang,[1] Xiaojuan Zhao,[1] Ying Zhang,[1] Wei Huang[1]
[1]Institute of Chemistry, Chinese Academy of Sciences, Beijing 100190, People's Republic of China
[2]University of Chinese Academy of Sciences, Beijing 100049, People's Republic of China
Correspondence to: X. Yang (E-mail: yangxin@iccas.ac.cn) and W. Huang (E-mail: huangwei@iccas.ac.cn)

ABSTRACT: A novel aromatic diamine-based benzoxazine (P-*m*PDA) is successfully synthesized from *m*-phenylenediamine (*m*-PDA), 2-hydroxybenzaldehyde, and formaldehyde. The polymerization behavior of P-*m*PDA and the properties of its thermoset are studied. The results indicate that P-*m*PDA owns favorable processability including low polymerization temperature, low liquefying temperature, and wide processing window. Even lower polymerization temperature (polymerization onset temperature as low as 80 °C) can be achieved by the promotion of catalysts. The ring-opening polymerization of P-*m*PDA first generates polybenzoxazine with *N, O*-acetal-type structure and arylamine Mannich-type structure, following which rearrangement from *N, O*-acetal-type structure to phenolic Mannich-type structure proceeds at elevated temperature. Furthermore, the polymerized P-*m*PDA shows outstanding performance such as extremely high glass transition temperature (T_g) of 280 °C, high char yield above 53% at 800 °C under nitrogen and excellent mechanical property. © 2016 Wiley Periodicals, Inc. J. Appl. Polym. Sci. **2016**, *133*, 43368.

KEYWORDS: properties and characterization; ring-opening polymerization; structure–property relations; thermosets

Received 13 November 2015; accepted 20 December 2015
DOI: 10.1002/app.43368

INTRODUCTION

Polybenzoxazines, obtained from the thermally activated ring-opening polymerization of 1, 3-benzoxazine monomers, are a novel class of thermosetting phenolic resins that are gaining increasing attention because of their unusual set of competitive material properties.[1–5] They combine typical properties of phenolic resins like high temperature resistance and high char yield with unique properties like low water uptake, high glass transition temperature (T_g), high stiffness, and excellent dielectric performance.[6–10] Furthermore, the polymerization of benzoxazines offers the benefits of producing no volatile byproducts and resulting in near-zero shrinkage materials.[11,12]

In general, the thermally induced ring-opening polymerization of benzoxazines produces polymers with phenolic moiety bridged by Mannich-type linkage [structure (i) in Scheme 1].[1,3,4] This structure allows the formation of various hydrogen bonds, especially the stable intra-molecular six-membered hydrogen bonds, which accounts for many unique properties of polybenzoxazines.[13,14] In addition to the Mannich-type linkage, another known structure in polybenzoxazine is the *N, O*-acetal-type linkage [structures (ii) and (iii) in Scheme 1], which has been found in the polymerization of some specific benzoxazines derived from phenols having blocked or sterically hindered ortho position and the benzoxazine/catalyst systems.[15–18] In most cases, the *N, O*-acetal-type linkage is labile and finally rearranges into the more stable Mannich-type linkage at elevated temperature.[17,18]

Although polybenzoxazines possess a variety of advantages, high ring-opening polymerization temperature, high liquefying temperature, and brittleness are the main drawbacks associated with typical polybenzoxazines. Further performance enhancement of polybenzoxazine is still strongly expected. To address these issues, the prevailing strategy has taken advantage of the inherent flexibility of benzoxazine synthesis, namely the condensation of abundant phenols, primary amines, and formaldehyde, to prepare various kinds of benzoxazines with desired and improved properties. One effective approach is preparing benzoxazine monomers containing another reactive group, such as aldehyde group,[19] alkynyl group,[20] allyl group,[21] epoxy group,[22] nitrile group,[23] carboxyl group,[24] maleimide group,[25] etc. Such functional groups would polymerize themselves or participate in the polymerization of benzoxazine, thus affording polybenzoxazines with improved thermal and mechanical properties, or sometimes lowered polymerization temperature. However, the corresponding phenols or primary amines from which the abovementioned benzoxazines derived are mostly not common

Additional Supporting Information may be found in the online version of this article.

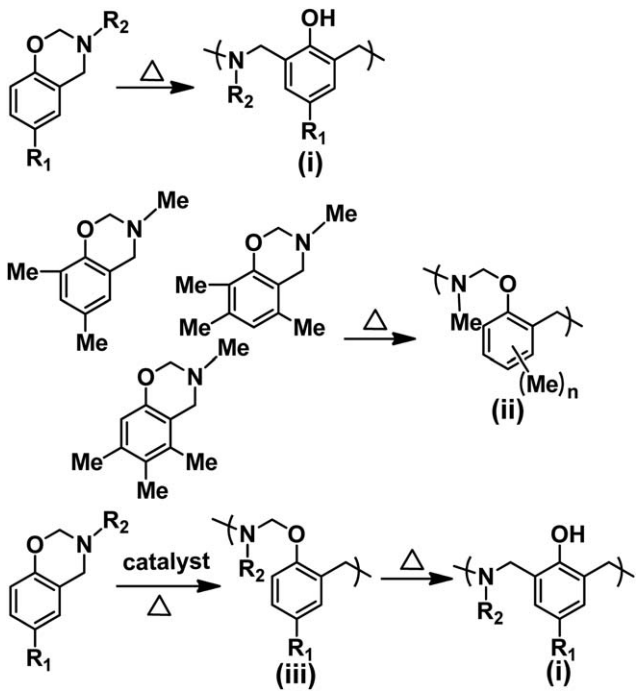

Scheme 1. Ring-opening polymerization of benzoxazines.

chemicals, therefore their widespread application is limited. Another effective approach is the incorporation of inert structural moieties like biphenyl,[26] fluorine,[27] naphthalene,[28] sulfone,[5] siloxane,[29] and polyether[30] to benzoxazines, which endows polybenzoxazines with desired high T_g, high toughness, low surface energy or favorable processability. In this case, the high polymerization temperature is still a problem awaiting solution.

Quite recently, Arnebold *et al.*[31] have reported a resorcinol-based benzoxazine with low polymerization temperature because of its specific structure which offered complex electronic effects. Inspired by the reported work, we prepared a novel *m*-phenylenediamine-based benzoxazine (P-*m*PDA) in this study, which was the isomer of resorcinol-based benzoxazine. The polymerization behavior of P-*m*PDA was investigated in detail, and the polymerization mechanism was proposed. The properties of P-*m*PDA's thermoset were systematically investigated and compared with the previously reported polybenzoxazines.

EXPERIMENTAL

Materials

Chloroform, ethanol and methanol were purchased from Beijing Chemical Works (Beijing, China); *m*-phenylenediamine (*m*PDA), formaldehyde (37% aqueous solution), 2-hydroxybenzaldehyde, 2-ethyl-4-methylimidazole (EMI), and *p*-toluenesulfonic acid (PTS) were supplied by Sinopharm Chemical Reagent (Beijing, China); zinc bromide ($ZnBr_2$) and sodium borohydride ($NaBH_4$) were obtained from J&K Scientific (Shanghai, China). All chemicals were AR grade and used as received without further purification.

Synthesis of P-*m*PDA

Synthesis of 1. *m*PDA (21.6 g, 0.2 mol), 2-hydroxybenzaldehyde (61.0 g, 0.5 mol), and ethanol (200 mL) were introduced into a 500 mL round bottom glass flask equipped with a magnetic stirrer. The reaction mixture was heated at 60 °C for 30 min. The precipitate was filtered, washed with ethanol and dried in a vacuum oven. A yellow powder 58.1 g (92% yield) was obtained.

^{1}H NMR (400 MHz, DMSO-d_6, δ): 13.00 (2H, OH), 9.06 (2H, H^7), 7.69 (2H, H^4), 7.54 (1H, H^{10}), 7.52 (1H, H^{11}),7.44 (2H, H^2), 7.37 (2H, H^3), 7.00 (4H, H^9 and H^1); ^{13}C NMR (100 MHz, DMSO-d_6, δ): 164.12 (C^6), 160.31 (C^7), 149.25 (C^8), 133.43 (C^{10}), 132.62 (C^2), 130.32 (C^4), 120.14 (C^3), 119.25 (C^9), 119.17 (C^5), 116.63 (C^1), 113.84 (C^{11}); FD-MS (*m/z*): calcd for $C_{20}H_{16}N_2O_2$, 316; found, 316. Anal. calcd for $C_{20}H_{16}N_2O_2$: C 75.93%, H 5.10%, N 8.86%; found: C 76.18%, H 5.11%, N 8.83%.

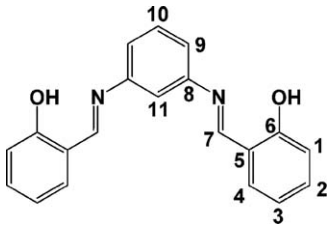

Synthesis of 2. Compound **1** (31.6 g, 0.1 mol) and methanol (600 mL) were introduced into a 1000 mL round bottom glass flask equipped with a magnetic stirrer. After $NaBH_4$ (15.2 g, 0.4 mol) was added, the reaction mixture was further stirred at room temperature for 10 h. The mixture was then poured into water with stirring, yielding a precipitate isolated by filtration. After the precipitate was dried, a gray powder 30.0 g (94% yield) was obtained.

^{1}H NMR (400 MHz, DMSO-d_6, δ): 9.42 (2H, OH), 7.16 (2H, H^4), 7.02 (2H, H^2), 6.77 (2H, H^1), 6.70 (3H, H^{10} and H^3), 5.89 (1H, H^{11}), 5.80 (2H, H^9), 5.59 (2H, NH), 4.10 (4H, H^7); ^{13}C NMR (100 MHz, DMSO-d_6, δ): 154.92 (C^6), 149.66 (C^8), 129.10 (C^{10}), 128.25 (C^2), 127.28 (C^5), 126.20 (C^3), 118.69 (C^4), 114.73 (C^1), 101.34 (C^9), 96.49 (C^{11}), 41.61 (C^7); FD-MS (*m/z*): calcd for $C_{20}H_{20}N_2O_2$, 320; found, 320. Anal. calcd for $C_{20}H_{20}N_2O_2$: C 74.98%, H 6.29%, N 8.74%; found: C 75.00%, H 6.38%, N 8.70%.

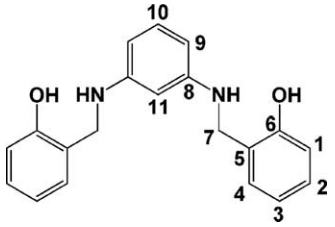

Synthesis of P-*m*PDA. Compound **2** (24.0 g, 75 mmol), 37% formaldehyde (12.2 g, 150 mmol), and chloroform (220 mL) were introduced into a 500 mL round bottom glass flask equipped with a condenser and a magnetic stirrer. The mixture was stirred at room temperature for 6 h and then further stirred at reflux temperature for 12 h. After that, the solution was dried

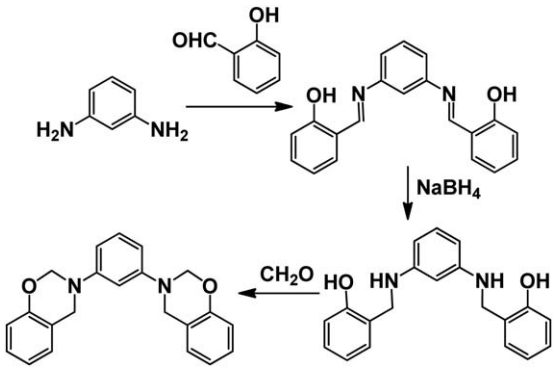

Scheme 2. Synthesis of P-*m*PDA.

over $MgSO_4$ and chloroform was removed using a rotary evaporator. A yellow viscous resin 25.5 g (99% yield) was obtained.

^{1}H NMR (400 MHz, DMSO-d_6, δ): 7.08 (5H, H^2, H^{11} and H^4), 6.88 (3H, H^1 and H^{12}), 6.72 (2H, H^3), 6.62 (2H, H^{10}), 5.42 (4H, H^8), 4.62 (4H, H^7); ^{13}C NMR (100 MHz, DMSO-d_6, δ): 153.95 (C^6), 148.81 (C^9), 129.60 (C^{11}), 127.58 (C^4), 127.08 (C^2), 121.36 (C^{12}), 120.40 (C^5), 116.21 (C^3), 109.75 (C^1), 107.04 (C^{10}), 78.73 (C^8), 48.96 (C^7); FD-MS (*m/z*): calcd for $C_{22}H_{21}N_2O_2$, 344; found, 344. Anal. calcd for $C_{22}H_{21}N_2O_2$: C 76.72%, H 5.85%, N 8.13%; found: C 76.31%, H 5.86%, N 8.43%.

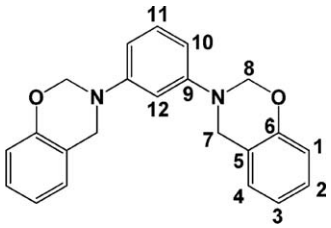

Polymerization of P-*m*PDA

After degassed under vacuum at 80 °C, P-*m*PDA was poured into a preheated stainless steel mold treated with a silicone-based mold-release agent, and was cured according to the following conditions: 150 °C for 2 h, 170 °C for 2 h, 190 °C for 2 h, 210 °C for 2 h and 230 °C for 2 h.

Characterization and Measurements

Fourier transform infrared spectroscopy (FT-IR) was performed on a BRUKER TENSOR-27 FT-IR spectrometer at room temperature in the range of 4000–400 cm^{-1}.

Nuclear magnetic resonance spectroscopy was performed on a BRUKER 400 NMR spectrometer in DMSO-d_6 at room temperature, with tetramethylsilane as external standard.

Field desorption mass spectrometry (FD-MS) was measured using a German Thermo Fisher DFS high resolution double focusing magnetic mass spectrometer, with German Linden CMS as ionic source.

Elemental analysis was determined using a Flash EA 1112 elemental analyzer.

Differential scanning calorimetry (DSC) was performed on a SII EXSTAR6000-DSC6220 instrument in N_2 flow of 50 mL min^{-1}, and at heating rates of 5, 10, 15, and 20 °C min^{-1}, respectively.

Thermogravimetric analysis (TGA) was carried out on a STA449F3 instrument at a heating rate of 10 °C min^{-1} in N_2 flow of 20 mL min^{-1}.

Parallel plate rheological measurement was performed using a TA AR-2000 rheometer under air atmosphere at a heating rate of 4 °C min^{-1} under an oscillatory shear mode with at a frequency of 1.5 rad s^{-1}. The plate diameter was 25 mm and the measuring gap was 1.0 mm.

Dynamic mechanical analysis (DMA) was performed on a TA Q800 instrument in the double-cantilever mode under air atmosphere at a frequency of 1 Hz and a heating rate of 5 °C min^{-1}. The dimensions of samples were 60 mm×12 mm×2.5 mm.

Flexural property was measured on an Instron Universal Tester Model 3365 (Instron, Canton, MA) at room temperature according to the China National Standard GB/T 16419-1996 in a three-point bending mode by using samples with dimensions of 80 mm×10 mm×4 mm, the span was 64 mm, and the strain rate was 1 mm min^{-1}. At least four specimens were measured and the obtained data were averaged.

RESULTS AND DISCUSSION

Synthesis and Characterization of P-*m*PDA

According to the type of phenols and primary amines used, the resulting benzoxazine monomers are mainly divided into two classes, diphenol-based and diamine-based. Generally, diphenol-based benzoxazines can be easily synthesized in solution or melt by the one-step condensation of phenols, primary amines and formaldehyde.[1,32,33] However, these methods are not applicable to the preparation of most of the aromatic diamine-based benzoxazines because the direct reaction of aromatic diamine and formaldehyde leads to the formation of insoluble triazine network. Aromatic diamine-based benzoxazines are now mainly prepared through the three-step method.[5] In this work, P-*m*PDA with high purity and yield was successfully synthesized by this method. The synthetic route is shown in Scheme 2.

Figure 1 shows the FT-IR spectrum of P-*m*PDA. Signal at 944 cm^{-1} was the characteristic mode of benzene with an attached oxazine ring. Absorptions at 1036 and 1227 cm^{-1} corresponded to the Ar-O-C symmetric and asymmetric stretching vibration, respectively. A band at 1365 cm^{-1} was attributed to the C-N stretching vibration. The appearance of these signals confirmed the presence of benzoxazine structure.

Figure 2(a) shows the ^{1}H NMR spectrum of P-*m*PDA. The characteristic resonances of oxazine ring assigned to the O-CH_2-N and Ar-CH_2-N methylene protons appeared as two singlets at 5.42 and 4.62 ppm, respectively. The multiplet at 6.5–7.3 ppm was attributed to the aromatic protons. The ratio of these peak areas obtained from ^{1}H NMR was in good agreement with the theoretical value.

Figure 2(b) shows the ^{13}C NMR spectrum of P-*m*PDA. The two characteristic resonances at 78.73 and 48.96 ppm were assigned to the methylene carbons of O-CH_2-N and Ar-CH_2-N in oxazine ring, respectively. No detectable resonances because of impurities were seen in the ^{1}H NMR and ^{13}C NMR spectra, suggesting that the prepared P-*m*PDA had high purity.

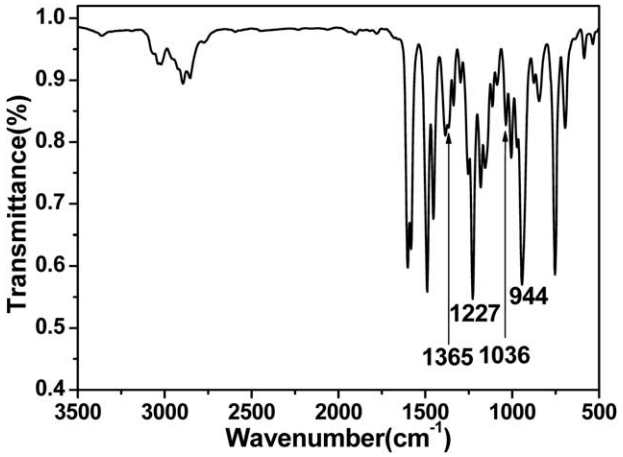

Figure 1. FT-IR spectrum of P-*m*PDA.

Polymerization Behavior of P-*m*PDA

To date, the known aromatic diamine-based benzoxazines were all solids with high melting temperatures (T_m) (as shown in Table I).[4,23,34] It was surprising to see that P-*m*PDA presented as a soft solid resin at room temperature, and no obvious melting transition was detected by DSC measurement. This was attributed to P-*m*PDA's irregular molecular structure, namely two benzoxazine groups locating at the meta position of benzene ring, which limited the crystallization of P-*m*PDA.

The polymerization of P-*m*PDA was monitored by rheological, DSC, and FT-IR. Firstly, the chemorheological behavior of P-*m*PDA was examined. The variation of dynamic viscosity of P-*m*PDA with temperature is shown in Figure 3. With the elevation of the temperature, the viscosity of P-*m*PDA dramatically dropped from 200 Pa s at 50 °C to 1 Pa s at 75 °C. After then, the viscosity continuously decreased below 0.2 Pa s and maintained this value from 95 °C to 165 °C. Sharp increase of viscosity was observed when the temperature was above 165 °C because of gelation. Compared with the reported typical aromatic diamine-based benzoxazines showing T_ms from 123 °C to 209 °C, P-*m*PDA had significantly low liquefying temperature and wide processing window, which were desired characteristics from the processing point of view.

The polymerization behavior of P-*m*PDA was then monitored by DSC as shown in Figure 4. A sharp exothermic peak centered at 193 °C was firstly observed, followed by a broad exothermic peak. Two interesting issues were worth noting in the DSC thermogram. Firstly, exothermic peak temperature (T_p) of P-*m*PDA was only 193 °C, which was 46–68 °C lower than the typical aromatic diamine-based difunctional benzoxazines listed in Table I. Unexpectedly, P-*m*PDA showed quite different characteristics from its isomer prepared from *p*-phenylenediamine, 2-hydroxybenzaldehyde, and formaldehyde which owned T_m of 180 °C and T_p of 260 °C.[34] Besides, the exothermic onset temperature (T_{onset}) of P-*m*PDA was only 160 °C, which was rarely seen for pure benzoxazines without initiators or additional functional groups.[31] It was speculated that the low polymerization temperature of P-*m*PDA was related to its molecular structure where two strong electron-donating tertiary amine structures of benzoxazine groups located at the meta position of benzene, basing on the report that electron-donating alkyl substituent group at the meta position of arylamine facilitated the ring-opening polymerization of benzoxazine at low temperature.[35] Secondly, DSC scan of most known benzoxazine monomers without other reactive group (such as these shown in Table I) gave typical single exothermic peak. However, in the case of P-*m*PDA, an obvious second exothermic peak appeared following the sharp peak, which was similar to the resorcinol-based benzoxazine.[31] This phenomenon may be the result of multiple polymerization or rearrangement reaction which has been described in literature,[16,36] and would be discussed later.

Now that P-*m*PDA owned low polymerization temperature, reasonably, if extra catalysts were added, even lower polymerization temperature can be achieved. Three catalysts including EMI, PTS, and $ZnBr_2$ were attempted here. DSC curves of P-*m*PDA with different catalysts are shown in Figure 4. As expected, these three catalysts promoted polymerization of P-*m*PDA effectively, and the corresponding T_{onset}s and T_ps were significantly lowered (listed in Table II). It was obvious that PTS and $ZnBr_2$ were

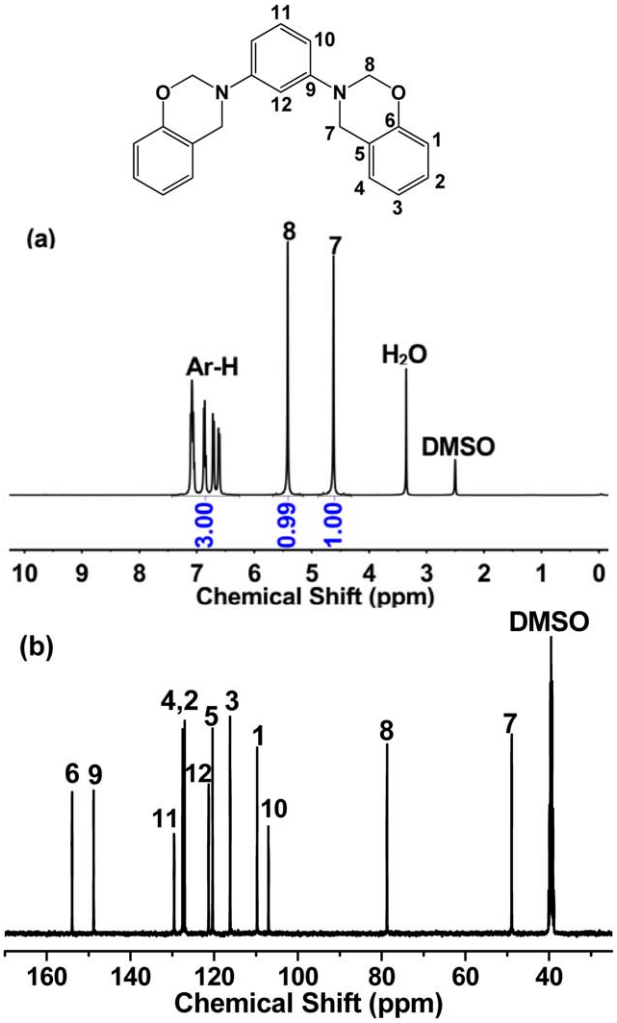

Figure 2. (a) ^{1}H NMR spectrum and (b) ^{13}C NMR spectrum of P-*m*PDA. [Color figure can be viewed in the online issue, which is available at wileyonlinelibrary.com.]

Table I. Properties of P-*m*PDA and Other Reported Benzoxazines

Ref.	Monomer Structure	T_m (°C)	T_p (°C)	$T_{5\%}$ (°C)	T_g (°C)	Char yield at 800 °C (%)
	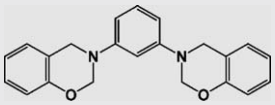	-	193	341	280	53
34	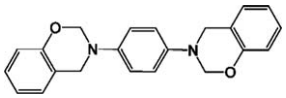	180	260	372	220	53
34	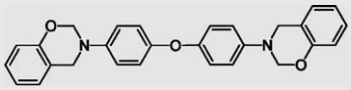	128	253[a]	376	194	52
4	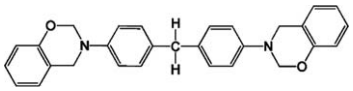	123	244	413	200	46
4	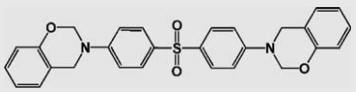	209	261	382	185	62
4	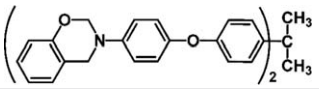	152	249	412	170	46
4	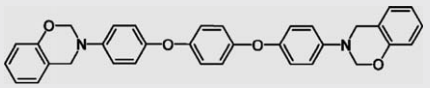	164	239	417	172	62
31	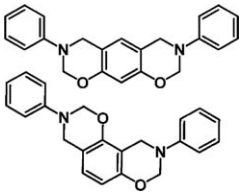	111, 146	179, 229	267	-	56n

[a] Data obtained from Ref. 23.
[b] Char yield at 600 °C.

more effective catalysts than EMI for P-*m*PDA polymerization, which lowered T_{onset}s about half. P-*m*PDA/PTS and P-*m*PDA/$ZnBr_2$ systems showed extremely low T_{onset}s around 80 °C, almost one of the lowest known polymerization temperature for benzoxazine systems.

Notably, two exothermic peaks were observed in all DSC curves in Figure 4, indicating that multiple polymerizations or rearrangement reaction happened during P-*m*PDA polymerization whether catalysts were added or not. [31] It had been proved that the rearrangement reaction from *N, O*-acetal-type structure to Mannich-type structure did happen for benzoxazines with EMI, PTS, and $FeCl_3$ as catalysts.[17,18] However, the multiple polymerization or rearrangement during polymerization was rarely reported for pure benzoxazines.[31,37] Therefore, the polymerization process of pure P-*m*PDA was examined in detail in this work.

Figure 5 shows the FT-IR spectra of P-*m*PDA after different polymerization stages. After heating for 2 h at 150 °C, signal corresponding to benzoxazine group at 944 cm^{-1} significantly weakened, while the signals at 1036 and 1227 cm^{-1} corresponding to the aryl ether structure were still obvious. This result suggested that most of the benzoxazine was consumed through the ring-opening polymerization and *N, O*-acetal-type structure was mainly formed after the first polymerization stage. With the proceeding of polymerization procedures, the absorptions at 1036 and 1227 cm^{-1} decreased gradually and disappeared after polymerization at 230 °C for 2 h. The *ortho*-substituted benzene absorption at 1489 cm^{-1} gradually vanished while the 1, 2, 3-

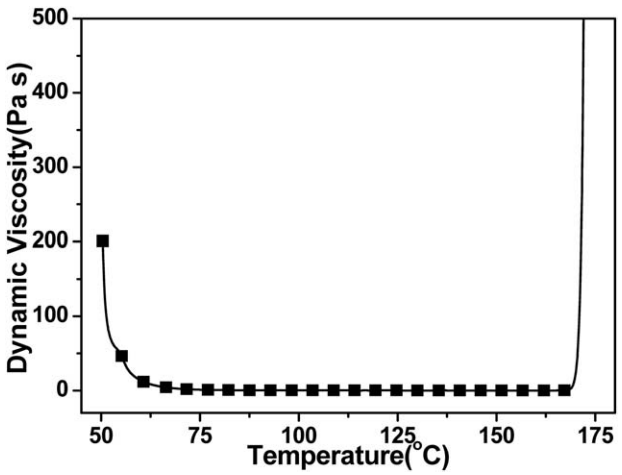

Figure 3. Rheological curve of P-*m*PDA.

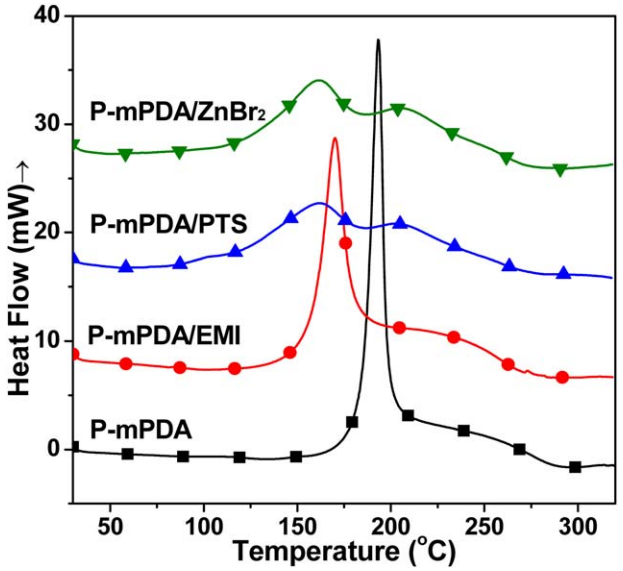

Figure 4. DSC curves of P-*m*PDA and P-*m*PDA/catalyst systems (10 °C min^{-1}). [Color figure can be viewed in the online issue, which is available at wileyonlinelibrary.com.]

trisubstituted benzene absorption at 1620 cm^{-1} arose and increased. What's more, the absorption at 1180 cm^{-1} attributed to C-N-C Mannich bridge structure and the absorption at 1264 cm^{-1} corresponding to Ar-OH gradually enhanced. These changes proved that the *N, O*-acetal-type structure [(iv) in Scheme 2] rearranged to the phenolic Mannich-type structure [(v) in Scheme 2] at the following polymerization stages. Another change worth noting was the signal at 690 cm^{-1} assigned to the *meta*-substituted benzene, which almost completely disappeared after the first polymerization stage, indicating that benzene ring of *m*PDA also participated in the ring-opening polymerization and arylamine Mannich bridge structure [(vi) in Scheme 2] was formed. In conclusion, for P-*m*PDA polymerization, structure (iv) and (vi) were mainly formed at the initial polymerization stage, and then (iv) rearranged to (v) at elevated temperatures. The polymerization mechanism of P-*m*PDA was proposed in Scheme 3.

Figure 6 shows the DSC curves of P-*m*PDA after different polymerization stages. With the proceeding of polymerization procedures, exothermic peaks gradually decreased and completely leveled off after heating at 230 °C for 2 h. It was noted that the sharp peak at lower temperature almost disappeared after the first polymerization stage. Combining this finding with the FT-IR result that most of the oxazine rings of P-*m*PDA were consumed after the first polymerization stage, the sharp peak in DSC curve was attributed to the reaction of ring-opening polymerization of P-*m*PDA, forming network with structure (iv) and (vi) as shown in Scheme 3. As a result, the following broad exothermic peak which diminished stepwise and vanished until 230 °C was because of the rearrangement reaction from structure (iv) to (v). The above results suggested that ring-opening polymerization of P-*m*PDA proceeded fast while the rearrangement reaction conducted in a much slower manner.

The polymerization kinetics was further studied by nonisothermal DSC to understand the reactivity of P-*m*PDA's polymerization better. Figure 7 shows the DSC curves of P-*m*PDA at different heating rates. As mentioned above, two overlapped exothermic peaks were observed in all DSC curves. The overlapped peaks were separated into two individual peaks, where the sharp peak at low temperature corresponding to the ring-opening polymerization reaction was noted as reaction 1, and the broad peak at high temperature corresponding to the rearrangement reaction was noted as reaction 2.

Table II. DSC Results of P-*m*PDA and P-*m*PDA/Catalyst Systems

Polymerization systems[a]	T_{onset} (°C)	T_{p1} (°C)	T_{p2} (°C)
P-*m*PDA	160	193	233
P-*m*PDA/EMI	120	170	217
P-*m*PDA/PTS	80	162	203
P-*m*PDA/$ZnBr_2$	80	162	205

[a] Catalyst content was 5 wt %.

As an exemplification, the experiment curve of P-*m*PDA at a heating rate of 10 °C min^{-1} together with the calculated curves of two resolved peaks were illustrated in Figure 8 (see Figures S1–S3 in Supporting Information for results at other heating rates). The corresponding T_ps of reaction 1 and reaction 2 are listed in Table III. With these data, the activation energies (E_as) of both reactions were calculated by Kissinger and Ozawa method according to eqs. (1) and (2), respectively[38]:

$$\ln\left(\frac{\beta}{T_p^2}\right)=\ln\left(\frac{Q_p AR}{E_a}\right)-\frac{E_a}{RT_p} \quad (1)$$

$$\ln\beta=\ln\left(\frac{AE_a}{R}\right)-\ln F(\alpha)-5.331-1.052\left(\frac{E_a}{RT_p}\right) \quad (2)$$

Figure 9 shows the Kissinger and Ozawa plots for reaction 1 and reaction 2. Through the slopes of these plots, Kissinger E_a

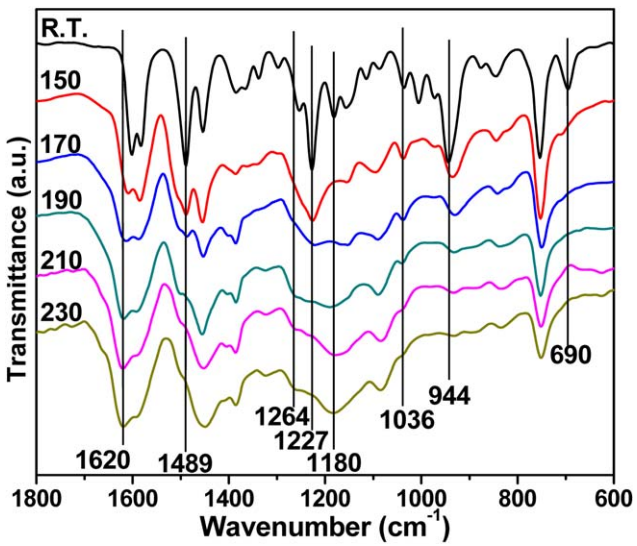

Figure 5. FT-IR spectra of P-*m*PDA after different polymerization stages. [Color figure can be viewed in the online issue, which is available at wileyonlinelibrary.com.]

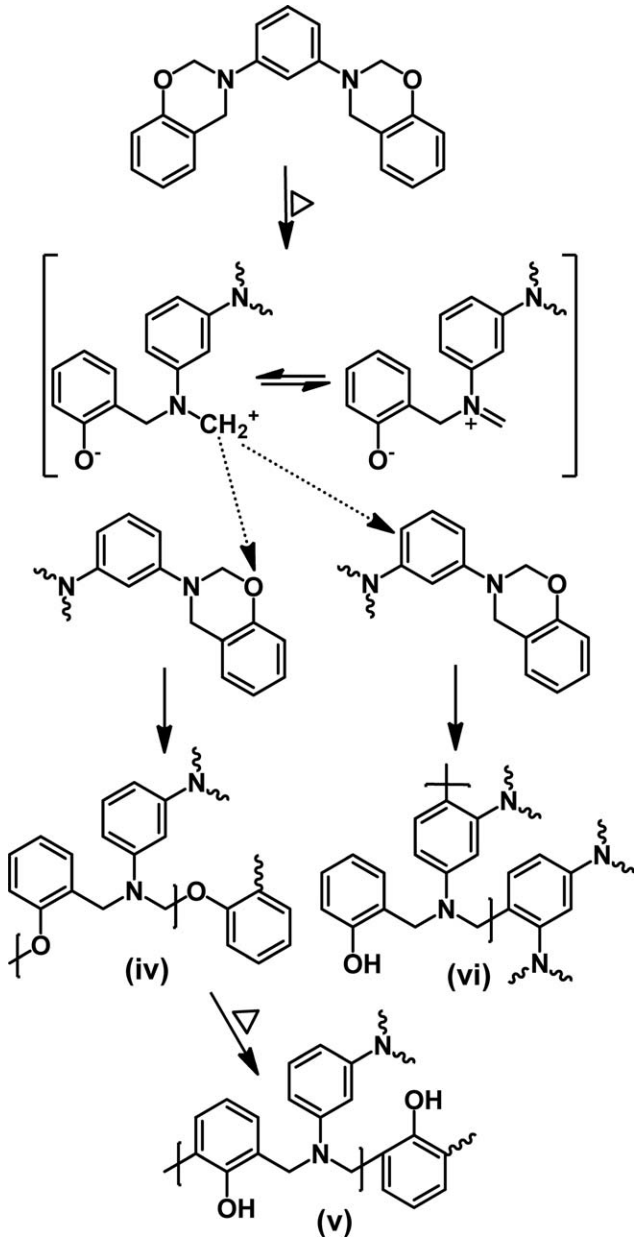

Scheme 3. Polymerization mechanism of P-*m*PDA.

and Ozawa E_a of both reactions were obtained, and the results are listed in Table III. The average values of Kissinger and Ozawa E_a for reaction 1 and reaction 2 were 77.9 and 110.0 kJ mol^{-1}, respectively. For reaction 1 which corresponded to the ring-opening polymerization of P-*m*PDA, the average E_a was lower than most of the reported benzoxazines,[38–41] indicating the high ring-opening reactivity of P-*m*PDA. As to reaction 2, the mechanism of which was the rearrangement reaction from *N, O*-acetal-type structure to Mannich-type structure, much higher E_a was observed, indicating that elevated temperature or long polymerization time was needed to achieve rearrangement.[17,18]

Properties of Polymerized P-*m*PDA

The mechanical and thermal prosperities of P-*m*PDA's thermoset (P-P-*m*PDA) were examined. Figure 10 shows the DMA

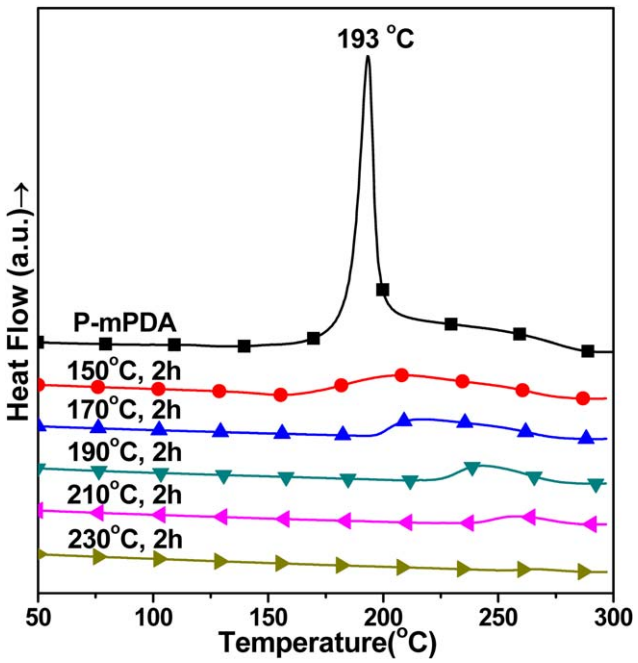

Figure 6. DSC curves of P-*m*PDA after different polymerization stages (10 °C min^{-1}). [Color figure can be viewed in the online issue, which is available at wileyonlinelibrary.com.]

curves of P-P-*m*PDA after different polymerization stages. The DMA curve of sample after the 150 °C polymerization stage was not given because of its poor strength. After the 170 °C polymerization stage, the resulting samples had enough strength for DMA measurements. The storage modulus (E') of these samples after each polymerization stage in the glassy region were significantly high as can be seen by the respective values above 4 GPa at 30 °C. The development of storage modulus (E') at 30 °C with the proceeding of polymerization procedures is shown in Figure 11. It was found that E' reached maximum after the 210 °C polymerization stage. The increase before 210 °C polymerization stage may be related to the rearrangement which led to

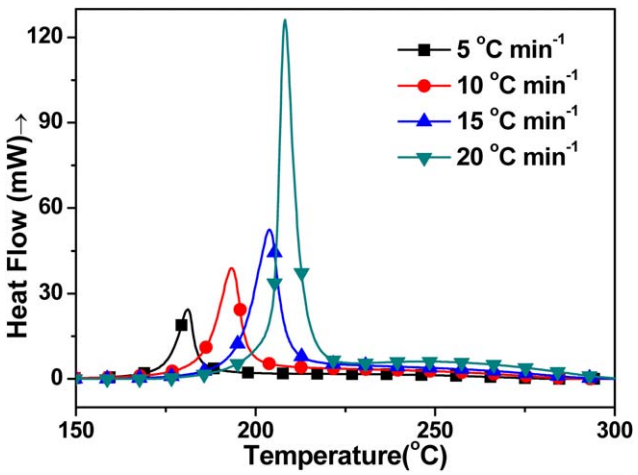

Figure 7. DSC curves of P-*m*PDA for different heating rates. [Color figure can be viewed in the online issue, which is available at wileyonlinelibrary.com.]

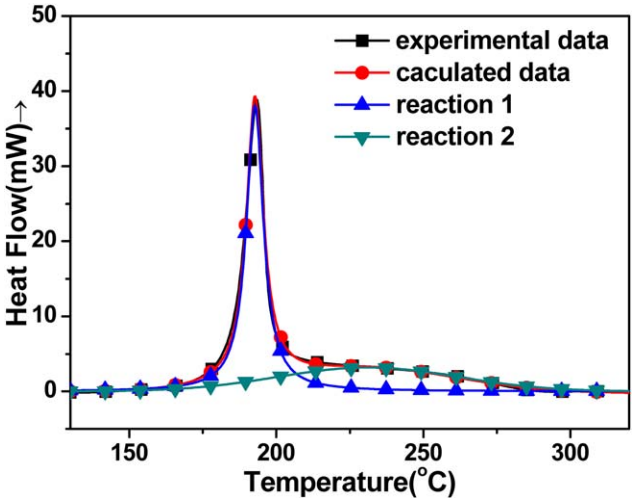

Figure 8. DSC curve of P-*m*PDA recorded at 10 °C min^{-1} and the corresponding calculated curves. [Color figure can be viewed in the online issue, which is available at wileyonlinelibrary.com.]

more hydrogen bonding formation, while the later decrease was caused by polymerization at higher temperature in air atmosphere which led to decomposition in some degree. However, the change of E' during the whole polymerization was small, indicating that the effect of rearrangement on E' was not as significant as expected.

Two obvious peaks were observed in the curve of dissipation factor for sample after the 170 °C polymerization stage, when the first peak appeared at 210 °C and the second peak appeared at 273 °C. As the polymerization procedure further proceeded, the second peak kept almost unchanged, while the first peak moved towards high temperature, became smaller, and finally merged with the second. Considering that P-P-*m*PDA was not a mixture, it was thought that the two peaks corresponded to different network structures, when the first was attributed to *N, O*-acetal structure and the second was attributed to Mannich-type structure. For the samples which exhibited two peaks, it was proposed that the samples actually owned one glass transition which corresponded to the first peak, and the second peak emerged because of the rearrangement happening during the heating process of DMA measurement. This rearrangement led to significant increase of T_g because of the formation of more hydrogen bonding from *N, O*-acetal-type structure to Mannich-type structure. The T_g of P-P-*m*PDA after the last polymerization stage was 280 °C as determined by the maximum of the dissipation factor.

The mechanical properties of P-P-*m*PDA after the last polymerization stage were also measured and compared with the

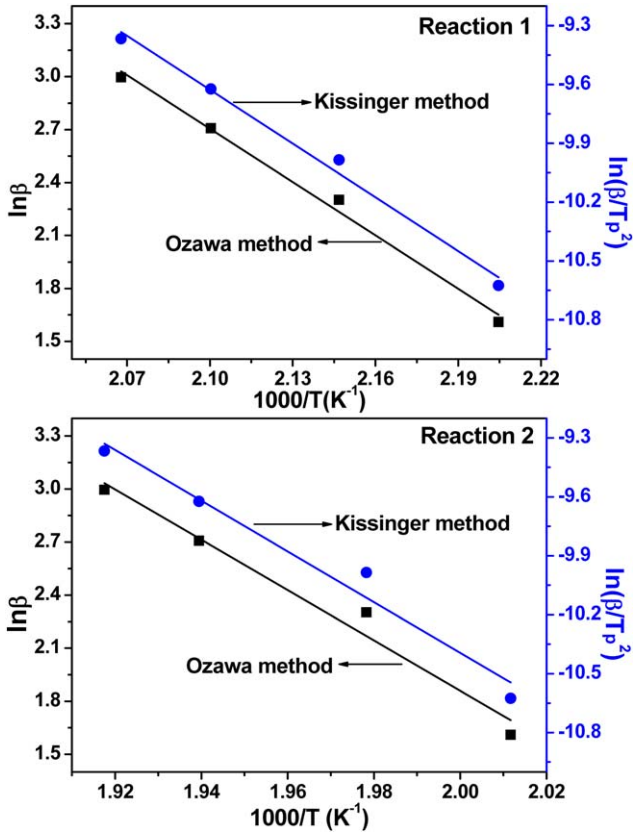

Figure 9. Ozawa and Kissinger plots for reaction 1 and reaction 2. [Color figure can be viewed in the online issue, which is available at wileyonlinelibrary.com.]

commercial bisphenol-A/aniline-type (Araldite MT35600, Huntsman) and bisphenol-F/aniline-type (Araldite MT35700, Huntsman) polybenzoxazines. The data list in Table IV showed that P-P-*m*PDA had much higher strength.

The thermal stability of P-P-*m*PDA after different polymerization stages was investigated by TGA as shown in Figure 12, and the corresponding data were listed in Table V. It was found that polymerization procedure had little effect on the thermal stability, and all samples had similar 5% mass loss temperatures ($T_{5\%}$) above 335 °C and char yields above 53% at 800 °C. This was because the rearrangement reaction happened before decomposition during TGA measurement. In other words, the measured samples in fact had almost the same network structure when decomposition began.

Some earlier reports have demonstrated that the derivative curve of TGA thermogram (DTG) provided useful information

Table III. T_ps and E_as of Reaction 1 and Reaction 2

	T_ps (°C) at different heating rates (°C min^{-1})						
Reactions	5	10	15	20	Ozawa E_a (kJ mol^{-1})	Kissinger E_a (kJ mol^{-1})	Average E_a (kJ mol^{-1})
Reaction 1	108.6	192.8	203.1	210.6	79.7	76.0	77.9
Reaction 2	224.1	232.5	242.6	248.5	112.6	107.3	110.0

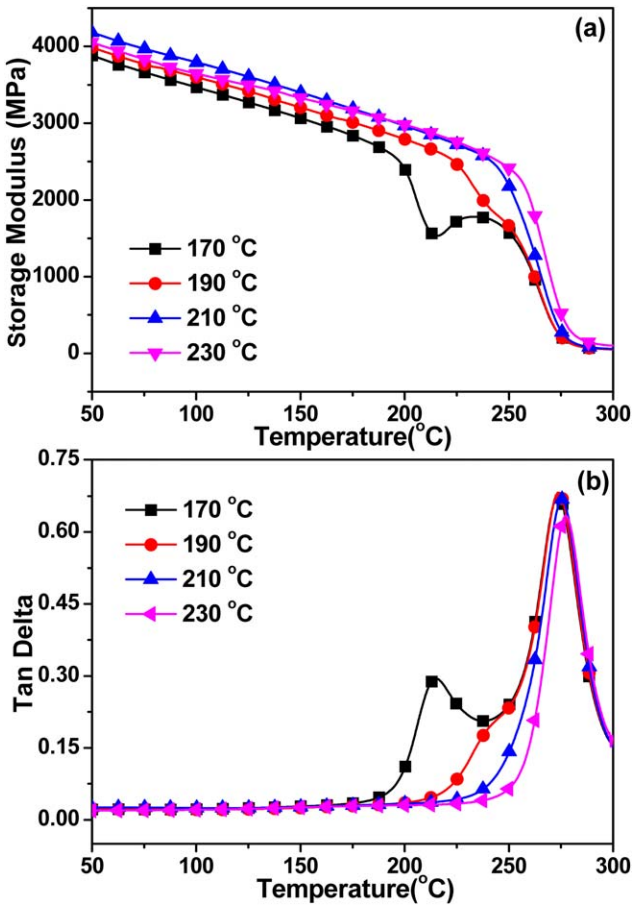

Figure 10. DMA curves of P-P-*m*PDA after different polymerization stages including (a) storage modulus and (b) dissipation factor. [Color figure can be viewed in the online issue, which is available at wileyonlinelibrary.com.]

about the network structure of polybenzoxazines.[18,42–45] Unlike the typical polybenzoxazine based on bisphenol-A and aniline (P-BA-a), of which DTG curve showed a three-stage degradation process,[18,43–45] P-P-*m*PDA presented a two-stage degradation process. The degradation happened at low temperature corresponding to the volatilization of aniline was not observed for P-P-*m*PDA, because the amine segment was introduced into the network by its own spacer groups and retarded the evaporation of the amine cleavage.[42] In P-P-*m*PDA's DTG curves, the first degradation process reached its maximum rate of 0.19% $°C^{-1}$ at 360 °C (T_{max1}) and the second showed a maximum rate of 0.12% $°C^{-1}$ around 450 °C (T_{max2}). The similar two-stage degradation process for samples after different polymerization stages was also the result of the rearrangement before decomposition during measurements.

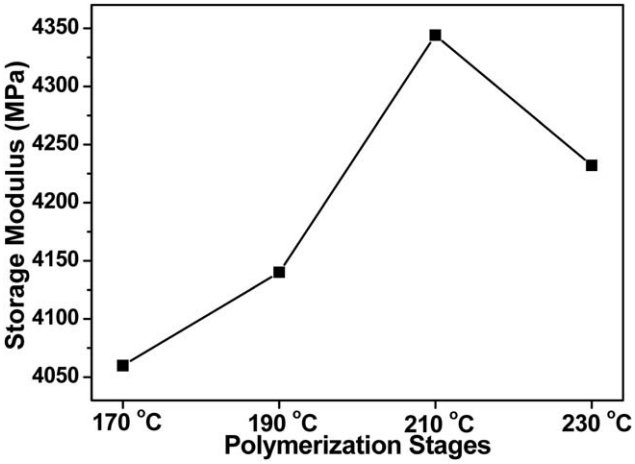

Figure 11. Storage modulus (E') of P-P-*m*PDA at 30 °C after different polymerization stages.

Table IV. Mechanical Properties Comparison of P-P-*m*PDA with MT35600 and MT35700

Polybenzoxazine	Flexural strength (MPa)	Flexural modulus (GPa)
P-P-*m*PDA	147 ± 26.3	5.5 ± 0.1
MT35600[a]	122	5.4
MT35700[a]	127	5.6

[a] Data were obtained from the Huntsman's technical datasheet.

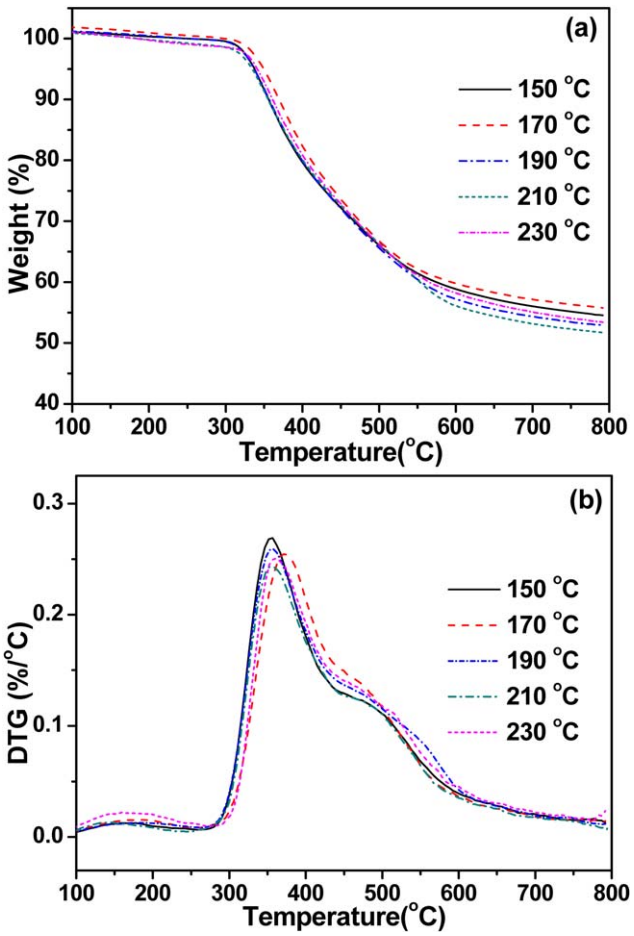

Figure 12. (a) TGA curves and (b) DTG curves of P-P-*m*PDA after different polymerization stages. [Color figure can be viewed in the online issue, which is available at wileyonlinelibrary.com.]

Table V. TGA data of P-P-*m*PDA after Different Polymerization Stages

Polymerization stages	$T_{5\%}$ (°C)	T_{max1} (°C)	Maximum rate 1 (%/°C)	T_{max2} (°C)	Maximum rate 2 (%/°C)	Char yield at 800 °C (%)
150 °C	336	355.5	0.20	447.2	0.12	54.5
170 °C	349	368.2	0.19	453.4	0.13	55.7
190 °C	337	356.6	0.20	449.6	0.13	53.0
210 °C	335	356.5	0.19	450.4	0.12	56.5
230 °C	341	363.7	0.19	457.1	0.12	53.4

Two benzoxazine isomers of P-*m*PDA have been reported before, and the thermal properties of polybenzoxazines from P-*m*PDA and its two isomers were compared in Table I. It was found that P-P-*m*PDA showed extremely higher T_g than polybenzoxazine from *p*-phenylenediamine. $T_{5\%}$ of P-P-*m*PDA was significantly higher than that of resorcinol-based polybenzoxazine, but lower than *p*-phenylenediamine-based polybenzoxazine. Similar high char yields were found for all the three polybenzoxazines. The above results indicated that molecular structure displayed significant impact on thermal properties of the resulting polymers, and P-P-*m*PDA had outstanding thermal resistance.

CONCLUSIONS

A novel P-*m*PDA was successfully synthesized, and the structure was confirmed by ^{1}H NMR, ^{13}C NMR and FT-IR. Because of the specific molecular structure, P-*m*PDA showed favorable processability such as low ring-opening polymerization temperature, low liquefying temperature and wide processing window. Through addition of PTS and zinc bromide ($ZnBr_2$), the polymerization onset temperature of P-*m*PDA can be decreased to as low as 80 °C. The polymerization behavior of P-*m*PDA was studied and the corresponding polymerization mechanism was proposed. The results indicated that the ring-opening polymerization of P-*m*PDA firstly happened, following which rearrangement reaction proceeded at high temperature from *N, O*-acetal-type structure to Mannich-type structure. Kinetic study proved that the activation energy of P-*m*PDA's ring-opening polymerization was lower than that of most reported benzoxazines. The polymerized P-*m*PDA owned excellent mechanical properties, high glass transition temperature (T_g) of 280 °C, and outstanding thermal stability including $T_{5\%}$ exceeding 335 °C and char yield at 800 °C exceeding 53%.

ACKNOWLEDGMENTS

This study is financially supported by the National Natural Science Foundation of China (No. 51303184).

REFERENCES

1. Ning, X.; Ishida, H. *J. Polym. Sci. Part A: Polym. Chem.* **1994**, *32*, 1121.
2. Ghosh, N. N.; Kiskan, B.; Yagci, Y. *Prog. Polym. Sci.* **2007**, *32*, 1344.
3. Takeichi, T.; Kano, T.; Agag, T. *Polymer* **2005**, *46*, 12172.
4. Lin, C. H.; Chang, S. L.; Hsieh, C. W.; Lee, H. H. *Polymer* **2008**, *49*, 1220.
5. Agag, T.; Jin, L.; Ishida, H. *Polymer* **2009**, *50*, 5940.
6. Kimura, H.; Murata, Y.; Matsumoto, A.; Hasegawa, K.; Ohtsuka, K.; Fukuda, A. *J. Appl. Polym. Sci.* **1999**, *74*, 2266.
7. Liu, Y. L.; Chou, C. I. *J. Polym. Sci. Part A: Polym. Chem.* **2005**, *43*, 5267.
8. Kim, H. J.; Brunovska, Z.; Ishida, H. *Polymer* **1999**, *40*, 6565.
9. Su, Y. C.; Chang, F. C. *Polymer* **2003**, *44*, 7989.
10. Yagci, Y.; Kiskan, B.; Ghosh, N. N. *J. Polym. Sci. Part A: Polym. Chem.* **2009**, *47*, 5565.
11. Ishida, H.; Allen, D. J. *J. Polym. Sci. Part B: Polym. Phys.* **1996**, *34*, 1019.
12. Ishida, H.; Low, H. Y. *Macromolecules* **1997**, *30*, 1099.
13. Kim, H. D.; Ishida, H. *J. Phys. Chem. A* **2002**, *106*, 3271.
14. Wirasate, S.; Dhumrongvaraporn, S.; Allen, D. J.; Ishida, H. *J. Appl. Polym. Sci.* **1998**, *70*, 1299.
15. Kim, H. D.; Ishida, H. *Macromolecules* **2000**, *33*, 2839.
16. Wang, Y. X.; Ishida, H. *Polymer* **1999**, *40*, 4563.
17. Sudo, A.; Kudoh, R.; Nakayama, H.; Arima, K.; Endo, T. *Macromolecules* **2008**, *41*, 9030.
18. Ran, Q. C.; Zhang, D. X.; Zhu, R. Q.; Gu, Y. *Polymer* **2012**, *53*, 4119.
19. Ran, Q. C.; Gu, Y. *J. Polym. Sci. Part A: Polym. Chem.* **2011**, *49*, 1671.
20. Kim, H. J.; Brunovska, Z.; Ishida, H. *Polymer* **1999**, *40*, 1815.
21. Agag, T. *J. Appl. Polym. Sci.* **2006**, *100*, 3769.
22. Andreu, R.; Espinosa, M. A.; Galia, M.; Cadiz, V.; Ronda, J. C.; Reina, J. A. *J. Polym. Sci. Part A: Polym. Chem.* **2006**, *44*, 1529.
23. Chaisuwan, T.; Ishida, H. *J. Appl. Polym. Sci.* **2010**, *117*, 2559.
24. Zou, T.; Li, S. F.; Huang, W. D.; Liu, X. L. *Des. Monomers Polym.* **2013**, *16*, 25.
25. Jin, L.; Agag, T.; Ishida, H. *Eur. Polym. J.* **2010**, *46*, 354.
26. Ning, X.; Ishida, H. *J. Polym. Sci. Part B: Polym Phys.* **1994**, *32*, 921.
27. Liu, J. P.; Ishida, H. *Polym. Polym. Compos.* **2002**, *10*, 191.

28. Shen, S. B.; Ishida, H. *J. Appl. Polym. Sci.* **1996**, *61*, 1595.
29. Zhu, C. L.; Wei, Y. Z.; Zhang, J.; Geng, P. F.; Lu, Z. J. *J. Appl. Polym. Sci.* **2014**, *131*, 40960.
30. Agag, T.; Geiger, S.; Alhassan, S. M.; Qutubuddin, S.; Ishida, H. *Macromolecules* **2010**, *43*, 7122.
31. Arnebold, A.; Schorsch, O.; Stelten, J.; Hartwig, A. *J. Polym. Sci. Part A: Polym. Chem.* **2014**, *52*, 1693.
32. Ishida, H. U.S. Patent 5,543,516, Aug 6, **1996**.
33. Sawaryn, C.; Landfester, K.; Taden, A. *Macromolecules* **2011**, *44*, 7668.
34. Chang, S. L.; Lin, C. H. *J. Polym. Sci. Part A: Polym. Chem.* **2010**, *48*, 2430.
35. Ishida, H.; Sanders, D. P. *Polymer* **2001**, *42*, 3115.
36. Liu, C.; Shen, D.; Sebastian, R. M.; Marquet, J.; Schonfeld, R. *Polymer* **2013**, *54*, 2873.
37. Lin, C. H.; Shih, Y. S.; Wang, M. W.; Tseng, C. Y.; Chen, T. C.; Chang, H. C.; Juang, T. Y. *Polymer* **2014**, *55*, 1666.
38. Ren, S. T.; Yang, X.; Zhao, X. J.; Zhang, Y.; Huang, W. *J. Appl. Polym. Sci.* **2015**, *132*, 41920.
39. Andronescu, C.; Garea, S. A.; Deleanu, C.; Iovu, H. *Thermochim. Acta* **2012**, *530*, 42.
40. Jubsilp, C.; Damrongsakkul, S.; Takeichi, T.; Rimdusit, S. *Thermochim. Acta* **2006**, *447*, 131.
41. Sponton, M.; Larrechi, M. S.; Ronda, J. C.; Galia, M.; Cadiz, V. *J. Polym. Sci. Part A: Polym. Chem.* **2008**, *46*, 7162.
42. Yang, P.; Gu, Y. *J. Appl. Polym. Sci.* **2012**, *124*, 2415.
43. Low, H. Y.; Ishida, H. *Polymer* **1999**, *40*, 4365.
44. Hemvichian, K.; Ishida, H. *Polymer* **2002**, *43*, 4391.
45. Low, H. Y.; Ishida, H. *J. Polym. Sci. Part B: Polym. Phys.* **1998**, *36*, 1935.